SQUIDs – Highly sensitive magnetic sensors

*M. P. Janawadkar, R. Baskaran, Rita Saha, K. Gireesan, R. Nagendran, L. S. Vaidhyanathan, J. Jayapandian and T. S. Radhakrishnan**

Superconducting Quantum Interference Devices (SQUIDs) are the world's most sensitive detectors of magnetic signals. Besides their use in the laboratory, they have a rich application potential in areas such as geophysics, biomagnetism and nondestructive testing of materials. A programme for the indigenous development of SQUID devices has been undertaken at the Indira Gandhi Centre for Atomic Research, Kalpakkam; high quality Josephson junctions, SQUID devices and large arrays of Josephson junctions have been successfully fabricated as a result of this effort. With the development of a low field SQUID magnetometer, the programme is poised to promote the indigenous development of SQUID based instruments for many applications.

THERE exist a large number of application areas where extremely small magnetic signals have to be detected and accurately measured. This requirement has been the major impetus for the development of magnetic sensors ranging from Hall probes (with a sensitivity ~ μT) to flux gate sensors (with a sensitivity ~ nT). With the advent of applied superconductivity, the last two decades have seen the introduction and utilization of Superconducting Quantum Interference Devices (SQUIDs) with a sensitivity ~ fT for the detection and characterization of the magnetic signals which are so small as to be virtually immeasurable by any other known sensor technology (Box 1). With the sensitivity realizable with the SQUID sensors it is possible, for instance, to measure the tiny magnetic fields produced by the nerve currents associated with the physiological activity of the human heart (magnetocardiogram – MCG) or the human brain (magnetoencephalogram – MEG); these signals have a typical strength ~ pT and introduction of SQUID sensors to characterize them has considerably enriched our understanding of both natural and evoked physiological responses. Some of the SQUID sensors have been designed to have energy sensitivity approaching Planck's constant. (The energy sensitivity is a figure of merit of the SQUID device and refers to the minimum signal energy per unit bandwidth (J/Hz) which must be coupled to the SQUID in order to generate an output just exceeding the noise. At 4.2 K, energy sensitivity of a typical DC SQUID sensor may be as low as 500 h; careful design and lower operating temperatures have enabled realization of the energy sensitivities approaching h). Thus SQUIDs constitute the most sensitive detectors of extremely tiny changes in magnetic flux. Taking into account the wide spectrum of application potential of SQUID devices (as also of the Josephson junctions on which these are based), a programme for indigenous development of

The authors are in the Materials Science Division, Indira Gandhi Centre for Atomic Research, Kalpakkam 603 102, India
*For correspondence (e-mail: tsr@igcar.ernet.in)

Box 1. Magnetic field sources and appropriate sensors

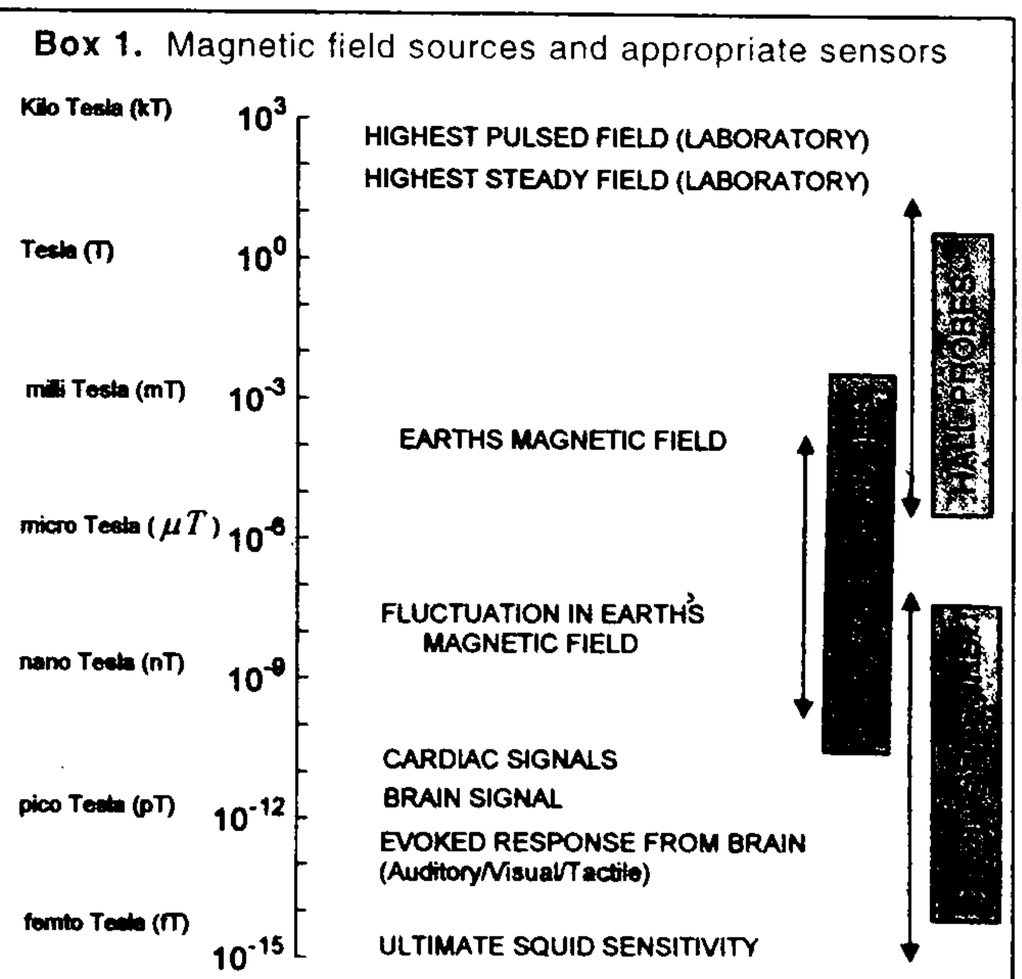

- *Hall probe:* Based on generation of Hall voltage in a semiconductor.
- *Flux gate:* A sinusoidal magnetizing current is passed through a coil surrounding a ferromagnetic core. Owing to nonlinearities of the magnetization curve of the core, output voltage of the pick-up coil contains different frequency components. The second harmonic component, which is proportional to external field, is phase sensitively detected. Feedback techniques are used to improve linearity.
- *SQUID:* Consists of a superconducting closed loop interrupted by Josephson junctions. Phenomena such as flux quantization and Josephson effect contrive to make the SQUID a transducer whose output voltage is a periodic function of magnetic flux. This periodic response is linearized using a flux locked loop electronics based on 100 kHz flux modulation and phase sensitive detection.

SQUID sensors was undertaken at the Indira Gandhi Centre for Atomic Research, Kalpakkam (IGCAR) a few years ago. As part of this programme, a complete range of laboratory-scale facilities have been set up at IGCAR for the design, fabrication and characterization of DC SQUID sensors. This superconducting device fabrication laboratory became functional in the early nineties with the commissioning of the basic equipment for thin film deposition by electron beam evaporation under ultra-high vacuum conditions and by RF magnetron sputtering technique in a class 1000 clean room environment as also the facilities for photolithographic patterning into device geometries with minimum feature sizes down to 2 μm under the class 100 laminar flow benches. A whole wafer sandwich process was selected for the fabrication of Nb–AlO_x–Nb Josephson junctions and devices based thereon since this process ensures contamination-free interfaces adjoining the tunnel barrier; this is crucial for the realization of high quality Josephson junctions. State-of-the-art DC SQUID sensors have been developed as a result of this effort and have been integrated into measurement systems using indigenously developed electronics and instrumentation. Emphasis has been placed on the generation of in-house expertise relating to all aspects such as device design, photomask making, device fabrication, testing and evaluation, instrumentation and the eventual utilization of devices for actual laboratory measurements. The laboratory is thus in a unique position to respond to the needs such as user-specific device configuration, on-chip integrated pick-up loop geometries, etc. besides being able to undertake the fabrication of other superconducting device structures starting with just the conceptual design. This article, which provides an update on an earlier one[1], surveys the progress that has already been achieved at Kalpakkam, and seeks to portray the potential of these devices for application in many areas in the national context; these include nondestructive testing of materials, geophysical explorations using the magnetotelluric methods, and a variety of exciting research in biomagnetism.

SQUID devices: Basic principles

The basic phenomena governing the operation of SQUID devices are flux quantization in superconducting loops and the Josephson effect. While detailed descriptions are already available in the literature[2,3], we include a brief account here if only to make the article self-contained. Although RF SQUID was historically the first device to be introduced and many of the commercially available SQUID magnetometers are based on the RF SQUID, we refer here exclusively to the DC SQUID which has since been shown to have a much higher sensitivity.

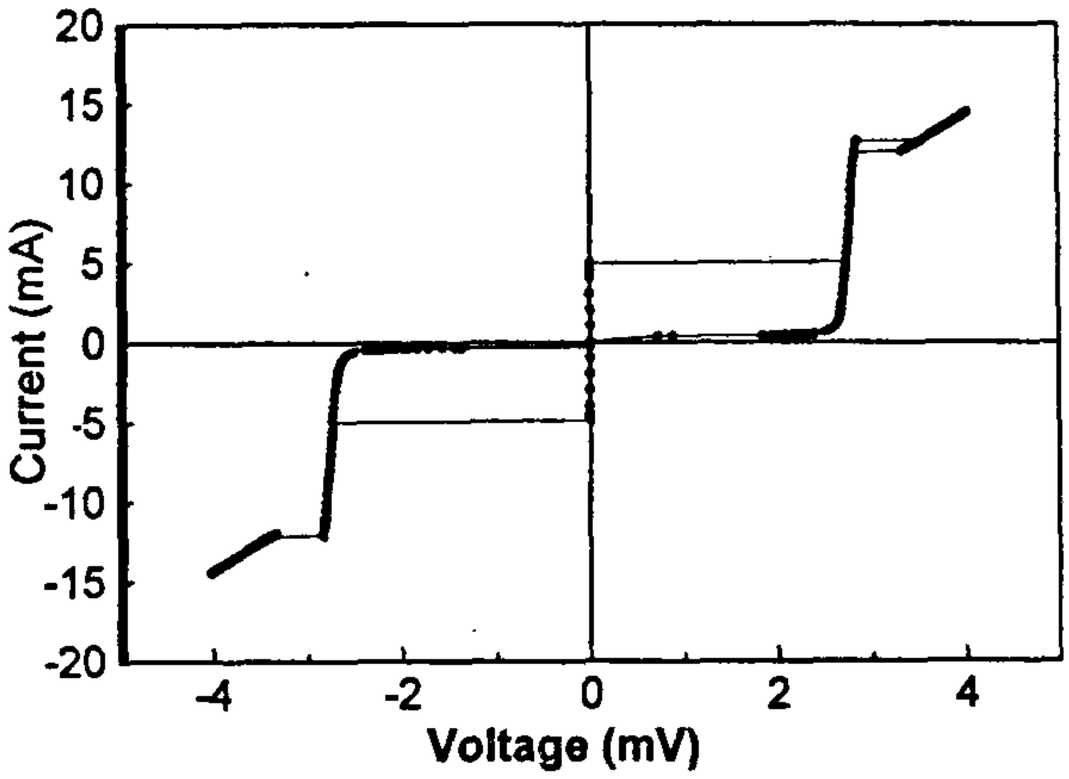

Figure 1. *I–V* characteristic of a typical Nb–AlO_x–Nb Josephson junction at 4.2 K. The junction has a V_m of 60 mV, comparable to the best junctions internationally reported.

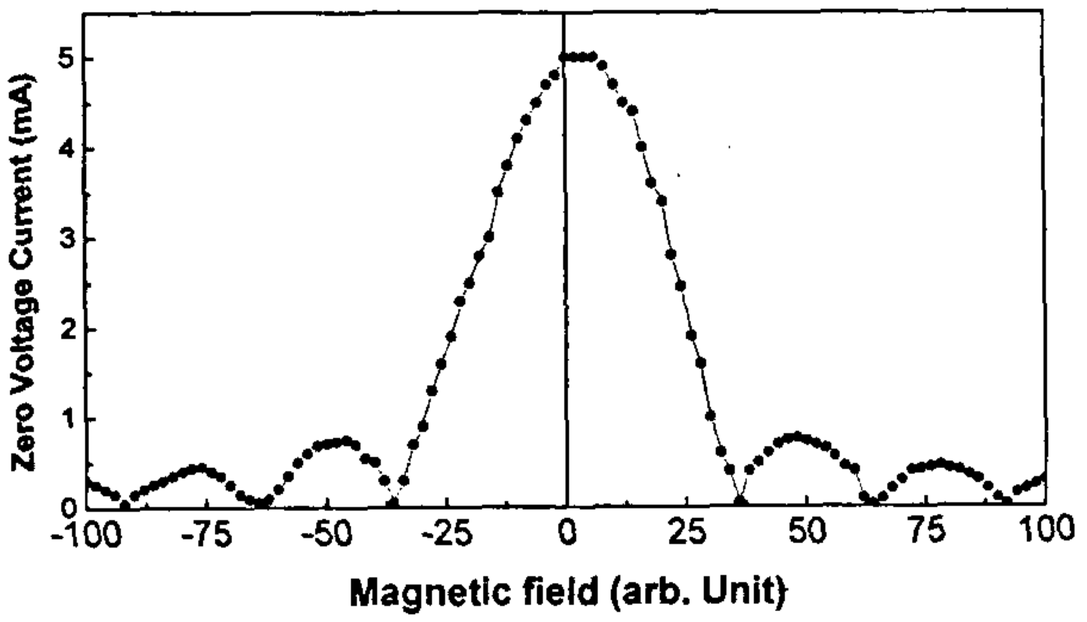

Figure 2. Dependence of critical current I_c of the junction on magnetic field.

The Josephson effect refers to the ability of two weakly coupled superconductors to sustain at zero voltage a supercurrent associated with transport of Cooper pairs, whose magnitude depends on the phase difference between the two superconductors. The maximum current which a Josephson weak link can support without developing any voltage across it is known as its critical current I_c. When the current passed through a Josephson weak link exceeds I_c, a voltage appears across it and the detailed nature of the *I–V* characteristic depends on the type of weak link. When the weak link is a tunnel barrier, the current phase relation is ideally sinusoidal ($I = I_c \sin\varphi$), and owing to substantial capacitance associated with the structure, the *I–V* characteristic is hysteretic as shown in Figure 1. This hysteresis may be eliminated by shunting the Josephson junction by a normal ohmic resistor *R*. For DC SQUIDs, one uses resistively shunted Josephson junctions with non-hysteretic *I–V* characteristics. When a small magnetic field is applied parallel to the plane of the junction, phase differ-

ence between the two superconducting electrodes varies linearly along a direction transverse to the direction of the magnetic field; this variation of phase difference causes supercurrents tunneling across different area elements of the junction to interfere and results in a variation of the critical current of the Josephson junction with applied magnetic field as shown in Figure 2. The dependence is analogous to the intensity variation in the context of the Fraunhofer diffraction at a single slit.

The DC SQUID consists of a closed loop of superconductor interrupted by two Josephson junctions. When a symmetric DC SQUID is biased with an external dc current I, a current $I/2$ flows through each of the two junctions; the critical current of the SQUID, in the absence of any external magnetic fields, is thus $2I_c$. When a magnetic flux Φ_{ext} is applied perpendicular to the plane of the loop, the loop responds with a screening current J to satisfy the requirement of flux quantization:

$$\Phi_{Tot} = \Phi_{ext} + LJ = n\Phi_0.$$

Here L is the inductance of the loop, n is an integer and Φ_0 is a flux quantum whose numerical value in SI units is 2×10^{-15} Wb. The screening current J is zero when the applied external flux is $n\Phi_0$ and is $\pm (\Phi_0/2L)$ when the external flux is $(n + 1/2)\Phi_0$, thus exhibiting a periodic variation with externally applied flux. The screening current J flowing around the SQUID loop leads to a reduction in the critical current of the SQUID from $2I_c$ to $(2I_c - 2J)$. The critical current of the SQUID is, therefore, a periodic function of externally applied flux. If the SQUID is biased with a current slightly larger than $2I_c$, the output voltage of the SQUID turns out to be a periodic function of the magnetic flux applied perpendicular to the plane of the SQUID loop as shown in Figure 3. The SQUID device thus functions as a transducer for magnetic flux producing measurable voltage changes at its output for small changes in magnetic flux applied at the input. Since the response of the SQUID is periodic, it is necessary to linearize it using the flux locked loop electronics in order to build SQUID-based measuring instruments.

The above account is necessarily naive and elementary. Detailed analysis[4] of the output voltage of the SQUID can be carried out taking into account phase dynamics of each resistively shunted junction in the presence of injected dc bias current, Nyquist current noise, and the applied magnetic flux. Such an analysis shows that the output noise is minimum when $2LI_c/\Phi_0 \approx 1$. When this condition is fulfilled, voltage modulation depth $\sim R/L$, where R is the dynamic resistance of the SQUID and the noise energy is given by $\varepsilon = 16kT\sqrt{LC}$, where C is the junction capacitance. To keep the noise energy low, one must therefore, have small area Josephson junctions (typically 3 μm × 3 μm) and low inductance SQUID loops (typically ~ 200 pH).

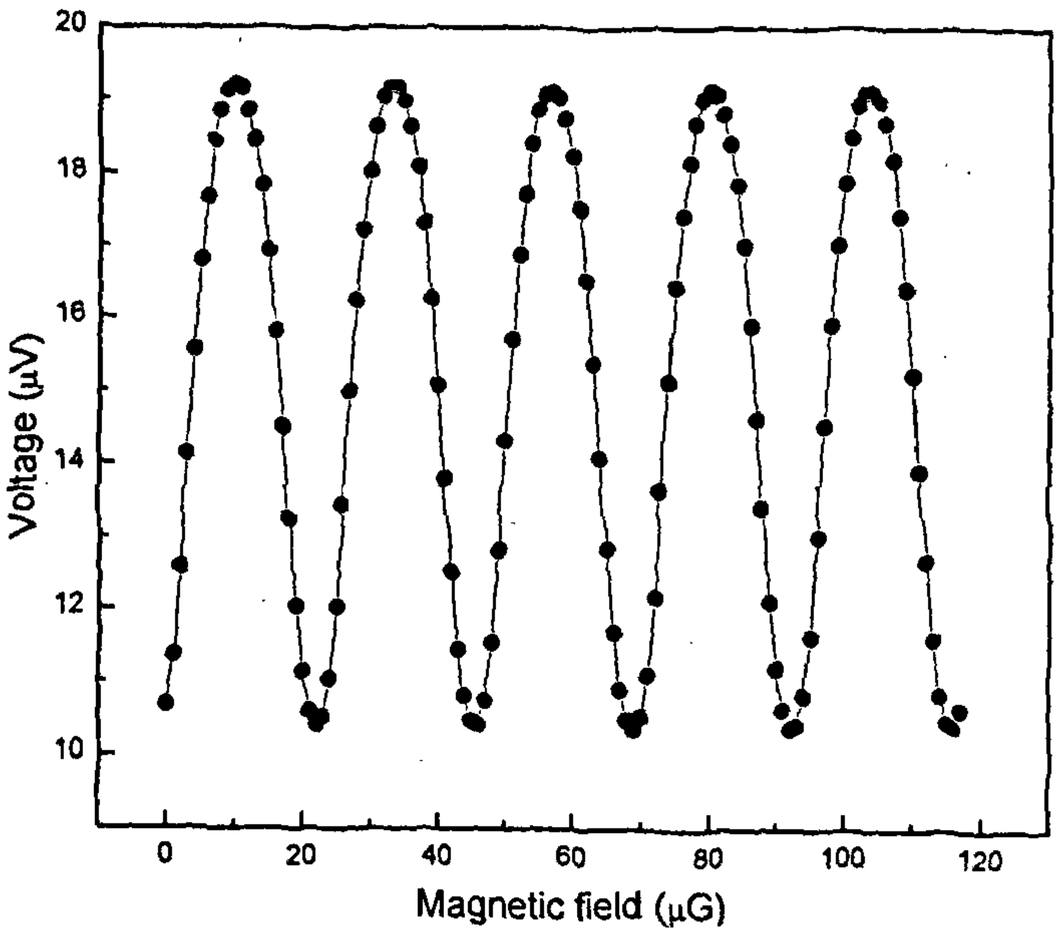

Figure 3. V–Φ characteristic of a typical DC SQUID. Output voltage is a periodic function of applied flux with the periodicity of a flux quantum Φ_0.

Design of SQUID devices

It is evident from the above that to realize lower noise figure, one ought to use junctions of small capacitance and SQUID loops of low inductance. An upper limit to the allowed inductance for the SQUID loop is obtained by requiring that the noise flux Φ_n associated with the circulating noise current i_n be much less than $\Phi_0/2$. Since, at temperature T, the noise energy $\frac{1}{2}Li_n^2 \sim kT$, it follows that $L << (\Phi_0^2)/(8\,kT)$. One typically uses SQUID loops with inductances ~ 100 to 200 pH. Owing to the small area of the SQUID loop, the bare devices even with the best flux resolution often have poor field resolution. To improve the field resolution it is customary to couple the SQUID to a superconducting flux transformer consisting of a large area pick-up loop and an input coil, which is tightly coupled to the SQUID loop (Figure 4). Any change in the magnetic field applied to the flux transformer results in a supercurrent, which flows into the input coil and couples flux in the sensing area of the SQUID. A field δB applied to the pick-up loop of area A_p and inductance L_p results in a screening current,

$$\delta i = \frac{\delta B A_p}{(L_p + L_i)},$$

where L_i is the inductance of the input coil (Figure 4). The flux $\delta\Phi$ coupled to the SQUID is given by

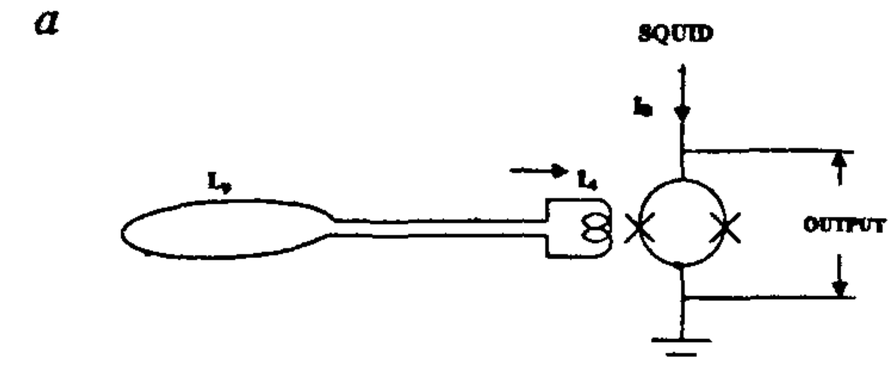

Figure 4. Superconducting flux transformer inductively coupled to the SQUID. *a* and *b* show the pick-up loop in the form of a magnetometer and a first order gradiometer respectively.

$$\delta\Phi = M\delta i = \delta B A_p \frac{M}{(L_p + L_i)},$$

where M is the mutual inductance between the input coil and the SQUID. In the presence of the flux transformer, the effective area of the SQUID is

$$A_{eff} = A_p \cdot \frac{M}{(L_p + L_i)}.$$

Minimum detectable flux $\Phi^{(p)}$ applied to the pick-up coil is the flux which results in a flux coupled to the SQUID just greater than its noise flux Φ_n:

$$\Phi^{(p)} = \frac{(L_p + L_i)}{M}\Phi_n = \frac{(L_p + L_i)}{\alpha\sqrt{L_i L}}\Phi_n,$$

where α is the coefficient of coupling between the input coil and the SQUID.

Equivalent noise energy $\varepsilon^{(p)}$ referred to the pick-up loop is

$$\varepsilon^{(p)} = \frac{[\Phi^{(p)}]^2}{2L_p} = \frac{(L_p + L_i)^2}{L_i L_p}\left(\frac{\Phi_n^2}{2\alpha^2 L}\right).$$

For a given SQUID device with a flux resolution Φ_n and loop inductance L, minimum value of $\varepsilon^{(p)}$ results when $L_i = L_p$.

The input coil is thus required to have an inductance matching that of the pick-up loop while remaining tightly coupled to the SQUID loop. As the size of the pick-up loop is large and that of the SQUID loop is very small, this matching, in general, becomes difficult.

An ingenious solution to this problem has been given by Ketchen and Jaycox[5]. Here, the superconducting loop consists of a flat washer with a central hole and a slit running from one end of the washer to the centre. The input coil is laid over this as a multiturn thin film spiral separated from the superconducting slit washer by an insulating layer. In this geometry SQUID inductance may be kept low by choosing the central hole of the slit washer to be sufficiently small while the number of turns in the spiral input coil may be increased to match the inductance of the pick-up loop. Despite its high inductance, the input coil is tightly coupled to the SQUID loop because of the special slit washer geometry: magnetic field produced by a current flowing through the input coil has to be calculated subject to the boundary condition that the normal component of magnetic induction at the surface of the superconducting washer must vanish. The boundary condition is best treated by the method of images; the image current under each turn of the spiral coil cannot cross the slit and is thus constrained to flow around the central hole resulting in what one might call a flux focussing effect and ensuring a tight coupling between the input coil and the SQUID. This geometry has been adopted practically universally ever since its introduction although some workers have based their design on other geometries such as the multiloop SQUID.

It may be noted that the pick-up loop of the flux transformer has to be individually optimized for each application taking into account the user-specific requirements such as field resolution, spatial resolution, etc. For geophysical applications, for instance, it is enough to target a good field resolution by increasing the size of the pick-up loop while for biomagnetism size of the pick-up loop has to be held small not only to improve the spatial resolution but also to minimize the detector size in a multi channel configuration. In most of the applications, it is also necessary to use pick-up loops in the form of a first or second order gradiometer in order to reject the ubiquitous magnetic noise from distant sources while detecting signals emanating from the desired sources.

Fabrication of Josephson junctions and SQUID devices

A Josephson junction consists of a thin tunnel barrier (AlO_x) with a thickness of just 1–2 nm sandwiched between two relatively thicker superconducting films (Nb). Since the superconducting transition temperature T_c of the deposited Nb films decreases very rapidly as a func-

tion of dissolved oxygen, it is necessary to ensure a low base pressure in the chamber before commencing the deposition of Nb films which have to be deposited at as high a deposition rate as possible. As a guard against possible contamination of both the interfaces adjoining the tunnel barrier, we have chosen to standardize the whole-wafer sandwich process for the fabrication of Nb–AlO_x–Nb junctions which involves deposition of Nb–AlO_x–Nb sandwich structure over the whole wafer without breaking vacuum and subsequent isolation of junctions by photolithography and reactive ion etching. While most of the workers have used sputtering as the deposition technique with a few isolated reports suggesting inferior junction quality on use of electron beam evaporation[6], we have shown that high quality Nb–AlO_x–Nb junctions can be produced with electron beam evaporation as well[7].

The fabrication begins with the deposition of 200 nm thick layer of Nb base electrode by electron beam evaporation after achieving ultra-high vacuum (5×10^{-10} mbar) in the chamber. After allowing a time duration ~ 1 h, a 5 nm thick Al film is deposited. The substrate is transported to another chamber where this freshly deposited aluminum layer is oxidized at room temperature by exposing it to pure oxygen at a pressure ranging between 1 and 10 mbar for 1 h. Tunnel current density of the Josephson junction is extremely sensitive to the thickness of the oxide barrier; the latter depends on the conditions under which the oxidation is carried out. After oxidation, the substrates are transported again to the main deposition chamber where a second aluminum layer having a thickness ~ 4 nm is deposited. Deposition of the trilayer is completed by a final deposition of ~ 60 nm of Nb film which forms the counter electrode of the junction.

From the trilayer deposited on the whole wafer without breaking vacuum, Josephson tunnel junctions and SQUID devices are fabricated by the Selective Niobium Etching Process (SNEP). First, the trilayer is structured into the appropriate base electrode geometry (e.g. slit washer for a SQUID device) by photolithographic patterning. The top niobium layer is then etched away by a reactive ion etching process based on CF_4 –5% O_2 plasma at all places excluding the specific locations where junctions are desired. A light anodization to a terminal voltage of 40 V is carried out to grow an insulation layer of anodic oxide on the base electrode as also the exposed edges by immersing the substrate in an electrolyte consisting of ammonium pentaborate, ethylene glycol and deionized water; anodization is carried out at constant current while monitoring the voltage developing across the anodization cell. An additional 400 nm of sputtered thin film of SiO_2 serves to provide further insulation around junctions. In this insulation layer, windows are opened at the location of the junctions by lift-off photolithography. Niobium layer of required thickness is then deposited and patterned to form counter electrode wiring. For SQUIDs a final layer of molybdenum is deposited and patterned to form the shunt resistor with a view to have junctions with non-hysteretic I–V characteristic.

By slight variations in this procedure we have fabricated high quality Josephson junctions, SQUID devices, DC SQUID gradiometers and arrays of Josephson junctions.

Characterization of Josephson junctions and SQUID sensors

To characterize the Josephson junctions and SQUID devices, they are usually mounted at the end of a dipstick equipped with several layers of mu-metal and a superconducting shield surrounding the sample holder. I–V characteristic may be measured by dipping the junction or the SQUID in a liquid helium dewar and noting the voltage developing across the device as the current passing through it is steadily increased starting from zero until a voltage ~ 5 mV is reached and then decreased. Figure 1 shows the dc I–V characteristic of a typical Josephson junction at 4.2 K indicating a clearly resolved energy gap structure at a bias voltage of 2.8 mV beyond which the quasiparticle conductance increases very sharply. The quality of the Josephson junctions is indexed by a parameter V_m, which is defined to be the product of the critical current of the junction and the subgap resistance measured at the bias voltage of 2 mV. At 4.2 K, some of the junctions fabricated attained values of V_m ~60 mV, which are comparable to the best values reported internationally. Dependence of the critical current I_C on the magnetic field applied parallel to the plane of the barrier is shown in Figure 2 revealing a near ideal Fraunhofer pattern.

These high quality junctions, after suitable shunting to eliminate hysteresis in the I-V characteristic, have been incorporated in DC SQUID sensors of both Ketchen–Jaycox and multi loop design. Figure 5 shows a photograph of a DC SQUID sensor with an integrated input coil based on the Ketchen–Jaycox design. The output voltage of the SQUID is a periodic function of applied magnetic flux as shown in Figure 3. Modulation depth typically ranges between 10 μV and 50 μV for a number of devices, which have been characterized; this is entirely adequate for their use as detectors of magnetic flux. Besides the modulation depth, it is usual to measure for each SQUID device parameters such as critical current, optimal bias current, dynamic resistance, mutual inductance between modulation coil and SQUID, mutual inductance between input coil and SQUID, effective area of the SQUID and spectral noise density as part of a detailed characterization.

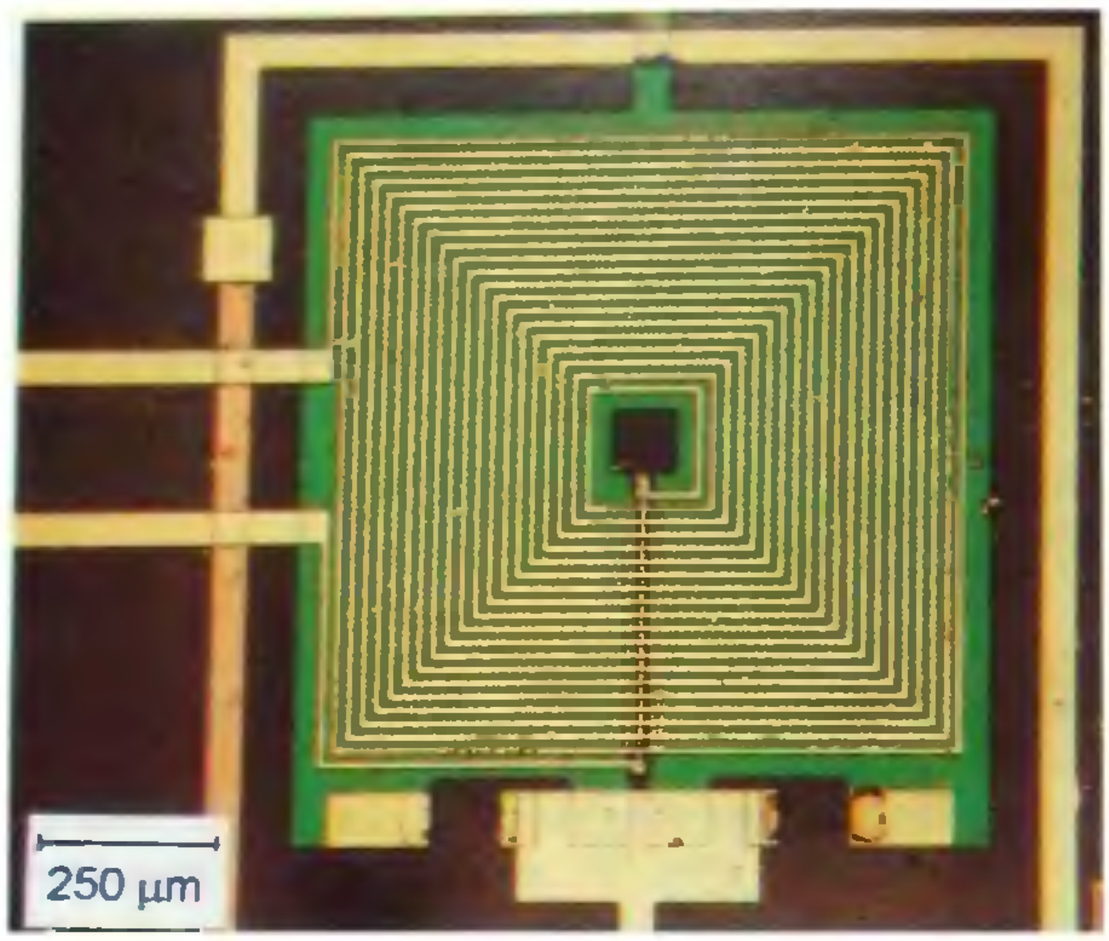

Figure 5. Photograph of a typical DC SQUID sensor based on the Ketchen–Jaycox design.

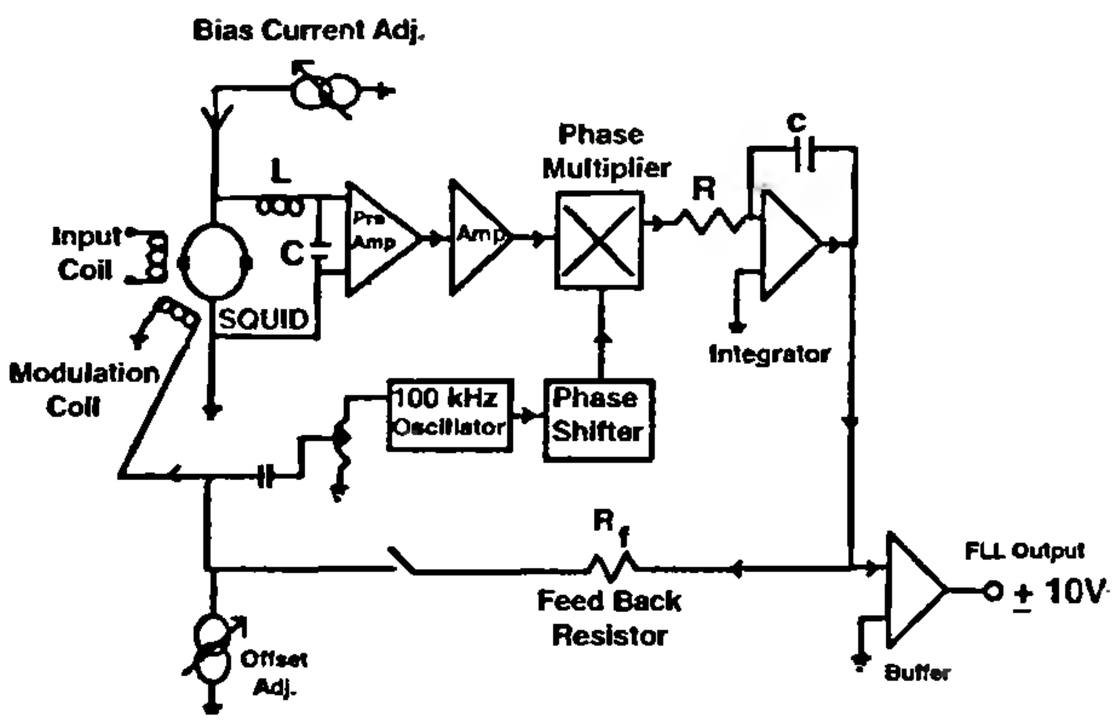

Figure 6. Block diagram of the flux locked loop electronics used to linearize the periodic response of the SQUID.

Flux locked loop electronics

Since the output of the SQUID device, viewed as a transducer of magnetic flux, is periodic rather than linear, it is necessary to employ a flux locked loop to linearize the output response for most, if not all, of the applications. A block diagram of the flux locked loop electronics is shown in Figure 6. An oscillator is used to modulate the flux coupled to the SQUID at a frequency of ~100 kHz and an amplitude $\sim\Phi_0/4$ by feeding appropriate current to the modulation coil. The signal appearing across the SQUID is phase sensitively detected at the modulation frequency after suitable amplification, and is fed back via a feedback resistor R_f, to the modulation coil. The voltage across the resistor R_f provides the SQUID read out. As long as the quasistatic flux threading through the SQUID loop remains on a peak or a trough of the periodic V–Φ characteristic, there is no signal at the modulation frequency present at the output. In the presence of a quasistatic signal applied additionally at the input, however, the circuit produces an output voltage which is proportional to the signal flux while ensuring that the SQUID stays locked in the vicinity of a single operating point on the V–Φ characteristic by generating a feedback flux which practically cancels the signal flux. This technique offers several distinct advantages: the signal of interest is moved to frequencies above the $1/f$ noise threshold of the preamplifier and there is a greater immunity from dc drifts in the amplifiers and the biasing circuitry. The closed loop signal bandwidth of the system is, of course, much less than the modulation frequency; however, a signal bandwidth of 1 to 10 kHz is considered adequate for a majority of applications. Such a signal bandwidth is realizable even in the presence of impedance matching devices such as a cooled LC resonant circuit or a cooled transformer which are often used in order to step up the low output impedance of the SQUID (typically 1 ohm) to values at which optimal preamplifier noise performance can be attained.

Figure 7 shows the spectral density of voltage noise recorded by feeding the flux locked loop output to the spectrum analyser. In the white noise regime, the observed voltage noise translates to a flux noise of $26\,\mu\Phi_0/\sqrt{\text{Hz}}$. Figure 8 shows the linearized output of the flux locked loop tracking low level low frequency magnetic signals deliberately coupled to the SQUID as part of the testing of the linearity of the flux locked loop circuit. Important characteristics of the flux locked loop circuit such as gain, dynamic range, slew rate and the spectral density of noise have also been evaluated.

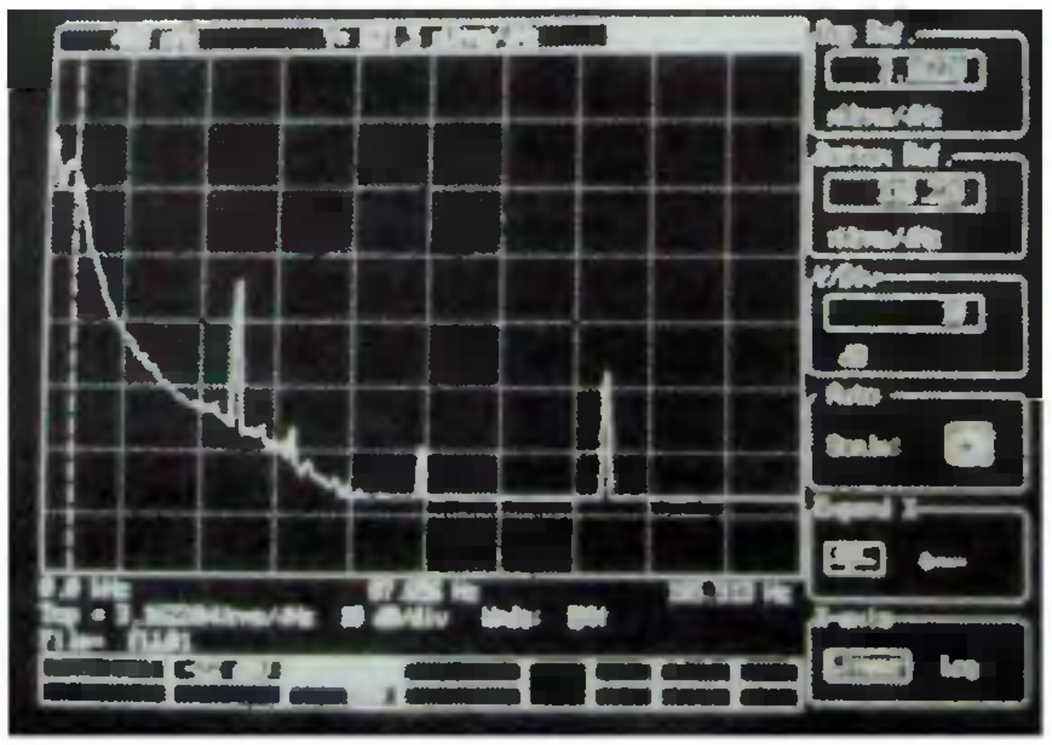

Figure 7. Spectral density of voltage noise of the SQUID at 4.2 K. x axis is frequency (20 Hz/div.); y axis is rms voltage noise (2 microVolts/div.)

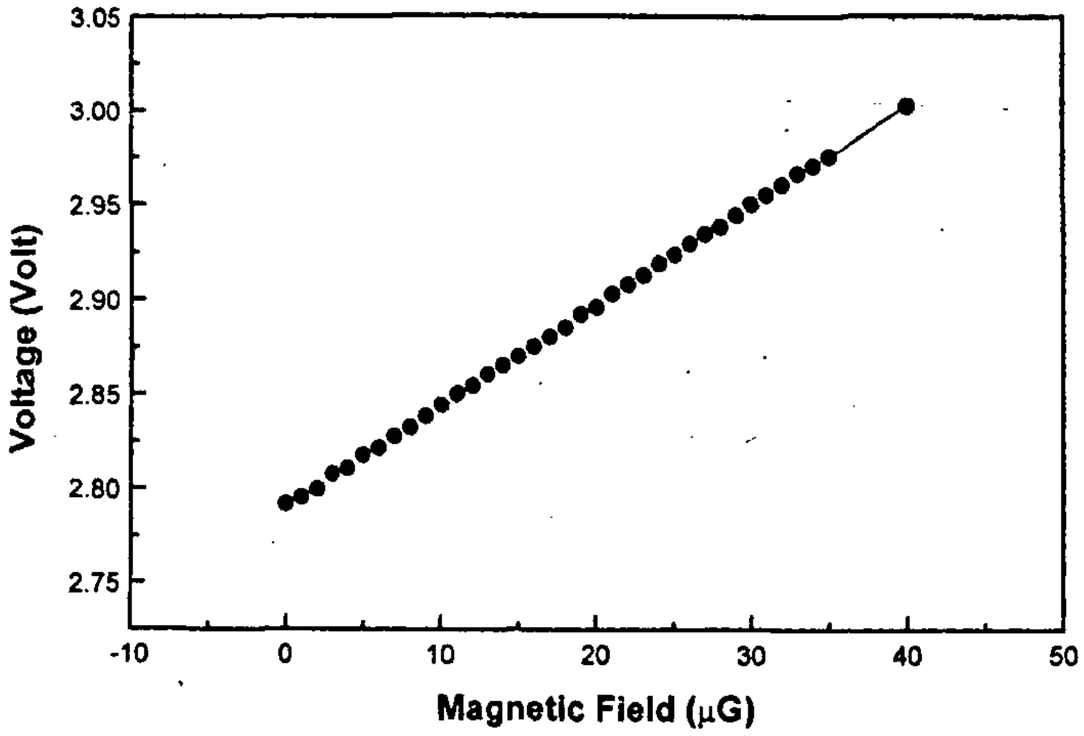

Figure 8. Linearized output of flux locked loop.

Development of a low field SQUID magnetometer

DC SQUID sensor and the flux locked loop electronics developed as described above have been used to measure the superconducting transition in materials such as lead, YNi_2B_2C, etc. Consequent to the Meissner effect-induced flux expulsion, the magnetic moment of the sample, induced by a small magnetising field, changes as the sample is driven across its superconducting transition. This change in magnetization induces a screening current to flow in the superconducting pick-up loop surrounding the sample; the pick-up loop is a part of the superconducting flux transformer, which couples the flux signal into the sensing area of the SQUID. The voltage output of the flux locked loop associated with the SQUID is then proportional to the magnetization change across the superconducting transition in the sample.

The apparatus used for this measurement is shown schematically in Figure 9. The sample is mounted in a variable temperature environment and is surrounded by a one turn pick-up loop of niobium wire which forms part of a first order gradiometer constituting the superconducting flux transformer inductively coupled to the SQUID device. The SQUID device, which is cooled to 4.2 K, is located in a separate enclosure shielded with the mu-metal and superconducting shields. A non-inductively wound heater serves to control the sample temperature, which can be varied at will by controlling the pressure of the helium exchange gas and the heater power. A magnetic moment may be induced in the sample by passing a dc current through a small solenoid surrounding the sample. To trap a stable magnetizing field, a superconducting shield surrounds the solenoid followed by several layers of mu-metal. Any change in

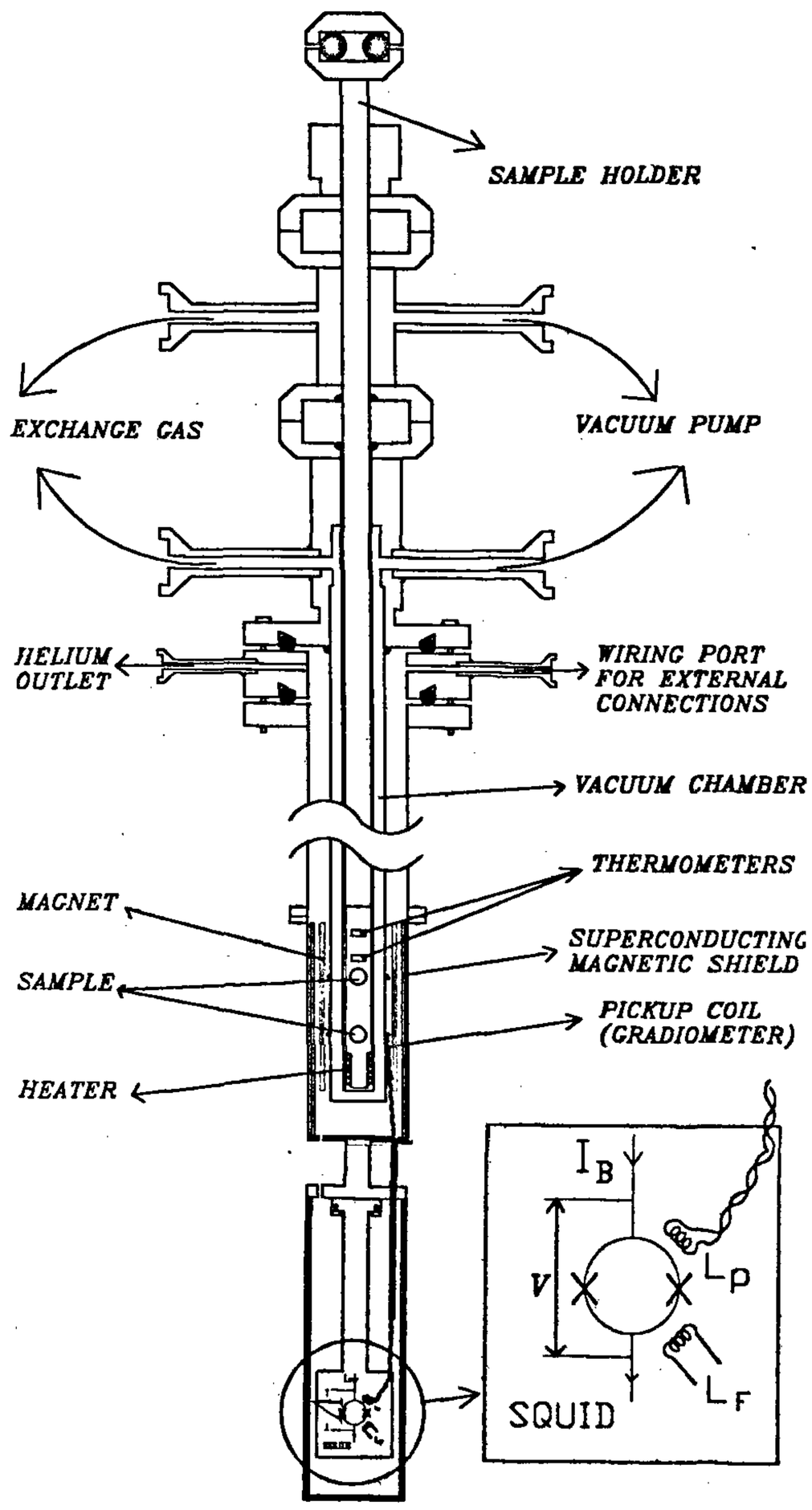

Figure 9. Schematic of the apparatus for measurement of superc ducting transition temperature T_c using SQUID. Inset shows lower portion at a higher magnification.

the magnetization of the sample (say across the sup conducting transition) induces a screening current in t superconducting flux transformer which couples it as signal flux into the sensing area of the SQUID. The fl locked loop electronics associated with the SQUID th generates an output voltage, which is proportional to t signal flux. Monitoring the output voltage of the SQU as a function of sample temperature enables one to tra changes in sample magnetization with temperature.

Figure 10 shows the superconducting transition in small sample of lead detected with the SQUID using t above apparatus. It is evident that the apparatus can

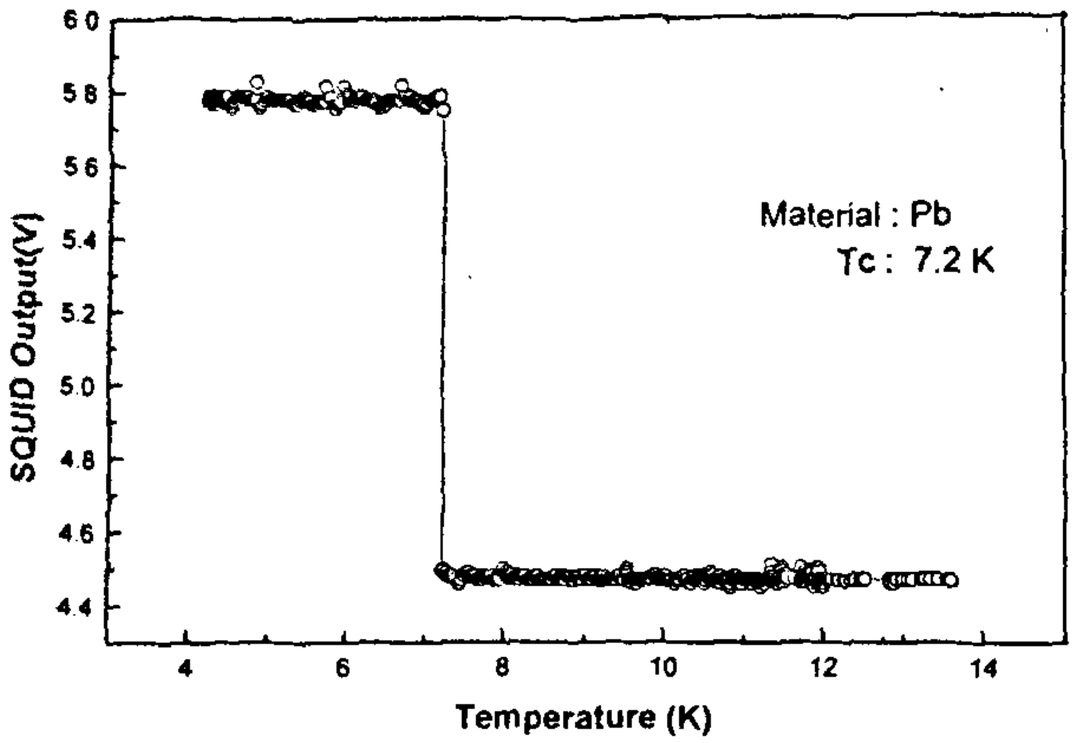

Figure 10. Superconducting transition in a specimen of lead detected with SQUID.

suitably configured to measure any physical quantity, which can be converted into a change in magnetic flux.

Application spectrum

SQUID devices have been used by several groups for carrying out a number of interesting studies in the laboratory. SQUID magnetometers have become the preferred work-horses for carrying out studies of magnetization as a function of applied magnetic field and temperature since standardized measurement systems are available from a number of commercial suppliers. Such studies have helped clarify the behaviour of vortices in superconducting materials including the High Temperature Superconductors (HTS). SQUIDs have been configured to measure extremely low-level voltage signals with a sensitivity approaching picovolts[8,9] depending on the source resistance. Use of SQUID devices has made possible studies involving low frequency NMR and NQR, and these have been recently reviewed[10]. They have also been used in a number of rather exotic experimental investigations including, for instance, detection of gravitational radiation[11], search for magnetic monopoles[12] and dark matter[13], etc. Here we focus on three areas of technological importance where the potential of SQUID devices has been amply demonstrated. Discussion here is necessarily brief and the interested reader is referred to recent review articles on applications of SQUID devices to geophysics[14,15], biomagnetism[16–18], and nondestructive testing[18,19] for additional details. Besides these, a number of applications of SQUID for defence are being discussed in the literature; these include the use of SQUID-based gravity gradiometry for navigation of submarines[20], for locating naval mines buried in sea bottom sediments[21], and for extra low frequency under water communications.

Application to geophysics

Development of experimental techniques for geophysical explorations has played a vital role in identifying, evaluating and utilizing the resources such as petroleum and hydrocarbons, minerals, geothermal energy, ground water, etc. hidden in sub-surface rock formations. Magnetic and electromagnetic fields are among the few probes (besides gravity gradiometry, seismic studies, etc.) available to the geophysicist to determine the properties of the earth's crust at depths of the order of 100 m to 10 km from the surface; the methods developed for the purpose include the resistivity, induced polarization, magnetotelluric, audio frequency magnetotelluric and controlled source electromagnetic methods. The magnetotelluric method, in particular, seeks to use the natural low frequency fluctuations in the earth's magnetic field (due to interaction with solar wind, lightning and thunderstorm activity) and the consequently induced electric fields to provide data on the resistivity distribution in the crustal material which can be interpreted, with suitable modelling, in terms of distribution of rock type and the subsurface geological structures. Accumulated empirical knowledge of the favourable rock types and geological structures capable of trapping oil and hydrocarbons has proved to be crucial in successful oil explorations. Although the method was proposed in the fifties, it was first used in USA in 1967, and today there are several companies, which offer contractual services for acquisition and interpretation of the magnetotelluric data. Unfortunately, much of the original data and procedures employed for the interpretation remain proprietary to the individual companies carrying out the survey, even when the interpretation is later confirmed by other complimentary techniques as well as actual drilling.

When the electromagnetic energy from the ionospheric and the thunderstorm activity is considered to be incident on the earth as a plane wave, it is partially reflected; the amplitude of the transmitted wave decays, typically on the length scale of a skin depth δ:

$$\delta(\text{km}) = 0.5\sqrt{\frac{\rho(\Omega\text{m})}{f(\text{Hz})}}.$$

The resistivity of rocks varies from ~ 1 Ωm to 10^4 Ωm depending on rock type, fluid permeating the rock pores (water with dissolved salts), fracture and faults, temperature, etc. It is evident that one needs a low frequency probe if one wishes to investigate deeper geological structures.

The components of the electric and magnetic fields are related by the earth's impedance tensor Z:

$$\begin{bmatrix} E_x \\ E_y \end{bmatrix} = \begin{bmatrix} Z_{xx} & Z_{xy} \\ Z_{yx} & Z_{yy} \end{bmatrix} \begin{bmatrix} H_x \\ H_y \end{bmatrix}.$$

The electric fields, typically ~10 mV/km are measured using electrodes grounded in a buffered copper sulphate electrolyte. For sensing the magnetic field components, typically ~pT, the conventional technique is to use an induction coil wound over a permalloy core, typically 1.5 to 2.0 m in length and 10 to 15 cm in diameter. Compared to the induction coils, SQUID devices offer lower noise figures, especially at low frequencies. The initial disappointment in not realizing the improvements in the quality of the magnetotelluric data after replacing the induction coils with the SQUID sensors has led to the introduction of techniques such as remote reference magnetotellurics; here an independent measurement of signals with a second SQUID device located several kilometres away is used to minimize the bias errors due to noise in the estimation of Z.

In the international scene, SQUID devices have been used in a number of magnetotelluric surveys with much improved sensitivity. Besides magnetotelluric studies they have been used for gravity gradiometry, study of tectonomagnetism (change in physical properties of stressed rocks in earthquake prone zone), etc. In India, widespread use of SQUID devices in geophysical explorations hinges on greater awareness about the potential of these devices, development of light weight and compact dewars, and flux locked loop electronics with a sufficiently high slew rate to permit deployment in field.

Application to biomagnetism

Biomagnetism refers to the study of tiny magnetic fields generated by nerve-currents which control the physiological activities of the human body in order to either study the functional aspects or to identify abnormalities caused by diseases. The strength of biomagnetic fields ranges from a few fT (evoked response from the brain) to a few nT (lung contamination by magnetic particles) and spans a bandwidth from near dc to ~1 kHz. SQUID devices have thus emerged as the only available biomagnetic sensors with a sensitivity adequate for this purpose and in recent years, multichannel SQUID-based instrumentation has been installed in several hospitals for clinical studies, especially magnetoencephalography (MEG), which is the magnetic analogue of electroencephalography (EEG). Indeed, while the EEG signals are affected by differences in the electrical conductivities of the scalp and the skull and their interpretation requires precise knowledge of thickness and conductivities of various layers, the magnetic fields measured with non-contact techniques are affected very little, if at all. Compared to Computer Assisted X-ray Tomography (CAT scans) and Magnetic Resonance Imaging (MRI), which provide static pictures of tissues, SQUID-based instrumentation provides dynamics of response and enables what may be called Magnetic Source Imaging (MSI) especially when one uses both the techniques with proper alignment of coordinates to derive information on locations of magnetic disturbances *vis-à-vis* actual anatomical structures. While SQUIDs have been used to monitor magnetocardiogram (MCG) to non-invasively localize cardiac arrhythmias, for foetal heart monitoring, etc. the scientific and commercial interests have largely concentrated on studies of the human brain (its normal alfa activity in 8–13 Hz bandwidth) evoked response, focal epilepsy, and other neurological disorders.

Using multichannel SQUID instrumentation, one usually measures the normal component of the magnetic field at a number of pre-selected points on a standard grid which lie on a plane parallel to the chest for cardiac studies or on a near spherical surface surrounding the head for brain studies. Electrical currents, which result from the ability of a cell membrane to alter its permeability to specific ions such as Na^+, K^+, Cl^-, etc. when stimulated, can often be modelled as current dipoles; current dipoles oriented parallel to the tissue surface are responsible for producing a magnetic field normal to the surface which may be measured by pick-up coils or sensors close to but outside the human body. Since only dipoles with a tangential component produce a normal magnetic field outside while the radial dipoles are externally silent, MEG is ideally suited for measuring electrical activity close to various fissures of the human brain; fortunately, however, most of the primary sensory areas of the brain such as auditory, visual, somatosensory, etc. are located within the fissures. It may be noted that the magnetic field due to a dipole in the measurement plane shows a maximum and a minimum; isofield contour maps help in locating the position (halfway between the measured extrema) and depth d of the dipole from the measurement plane ($d = \Delta/\sqrt{2}$, where Δ is the separation between the measured extrema). As d increases, however, large wave vector components in the magnetic field signal are selectively attenuated by the increased distance between the dipole and measurement plane, and it becomes difficult to reliably infer the location of the equivalent current dipole from measured spatial variation of the magnetic field. Nevertheless, a spatial accuracy of 1 to 2 mm in locating a current dipole is often attainable in MEG.

All current sources are not necessarily dipolar and in such situations, it becomes difficult to ascribe significance to an 'equivalent current dipole' inferred from measured magnetic field distribution. It then becomes necessary to determine the actual source current distribution from the measured magnetic field. It is, however, well-known that while fields can be uniquely calculated if a source current distribution is specified, the inverse problem does not admit of a unique solution in general. Progress in modelling can be made by taking into ac-

count realistic constraints based on known anatomical or physiological features.

Since the biomagnetic signals are weak, they are usually measured inside considerably expensive magnetically shielded rooms. Use of first or second order gradiometers has helped reduce the stringency of the shielding requirement. Necessity of having to measure the magnetic fields at a large number of locations simultaneously has led to development of multichannel SQUID instrumentation with as many as 122 channels at the Helsinki University of Technology, Finland and 256 channels at the Superconductor Sensor Laboratory, Japan. In India, liquid helium is already being used in several hospitals equipped with MRI machines. Widespread use of SQUIDs for biomagnetism will thus depend on emergence of specific clinical applications and reduction in cost per channel.

Application to non-destructive testing

Nondestructive testing (NDT) refers to techniques, which are used to detect, locate and assess defects, or flaws present in materials or fabricated components without affecting in any way their continued usefulness or serviceability. The defects may either be intrinsically present as a result of manufacturing processes or may result from stress, corrosion, etc. to which a material or a component may be subjected during actual use. It is evident that techniques to detect critical flaws before they have grown unacceptably large will be of vital importance in the industry for in-service inspection, quality control and failure analysis. Electromagnetic techniques such as eddy current testing are presently being routinely used in the industry to characterize the flaws. SQUID-based NDT, which made its debut in 1985, primarily aims at measuring magnetic fields at the location of either the SQUID device or the superconducting pick-up loop which is placed in close proximity to the sample under investigation; scanning techniques are used to map the magnetic field distribution from which one needs to infer the spatial distribution of the sources. The distance between the sensing element, which is at cryogenic temperatures, and the material or component under investigation, which is at room temperature, is referred to as the stand-off distance; a low stand-off distance (say 2 to 3 mm) is mandatory if one wishes to improve the accuracy with which the sources may be localized from the measured magnetic field distribution. Sources responsible for magnetic fields detected by the SQUID could be

(i) galvanic currents flowing in a specimen undergoing corrosion;
(ii) magnetization induced in localized regions of thermally aged specimens;
(iii) ac or dc electrical current directly injected in the specimen through electrical contacts;
(iv) eddy currents induced in the specimen by a coil carrying an ac current.

In the conventional eddy current testing, an ac current at 100 kHz to 10 MHz is used to induce eddy currents in a specimen. Defects and flaws present in the specimen influence the distribution of eddy currents and give rise to a measurable change in the impedance of the inducing coil. Since the ac fields decay over the length scale of a skin depth, the method is limited to detection of near-surface flaws in a conducting specimen. If one lowers the frequency to increase the skin depth, signal amplitude decreases, making it difficult to maintain a good signal-to-noise ratio. Use of SQUID devices eliminates this limitation by providing a high sensitivity at low frequencies. This high sensitivity makes it possible to design superior systems for detection of magnetic anomalies even after making engineering compromises and trade-off. The low frequency sensitivity of the SQUID device enables one to detect deep sub-surface flaws undetectable by the conventional eddy current testing owing to skin depth limitations; besides, their ability to function down to dc enables one to map slowly varying weak galvanic currents responsible for corrosion damage. Wide dynamic range of the SQUID implies that the ability to monitor extremely small changes in magnetic fields persists even in the presence of relatively large dc magnetic fields.

SQUID devices have been used to detect cracks and corrosion damage in specimens ranging from a simulated lap joint in an aircraft wing to a ship hull plate having a surface breaking fatigue crack. They have been used to develop new inspection tools for printed circuit boards and integrated circuits by exploiting their ability to monitor distribution of currents. Their widespread use in NDT is dependent on finding a suitable niche in the industry, wherein SQUID-based NDT can be used with advantage over the conventional NDT techniques, and development of improved mathematical models not only for inferring the source current distributions but also for correlating the measurements to specific types of defects and their size.

Conclusions

A self-contained superconducting device fabrication and characterization laboratory has been set up at Kalpakkam and Nb–AlO_x–Nb Josephson junctions and SQUID devices comparable to the ones available on the international scene have been fabricated. This development marks the realization of an important enabling technology and offers the possibility of embarking on any of a number of applications mentioned earlier. While work is

on hand to build several systems for laboratory use, it may be possible to realize a wide spectrum of applications through initiatives of interested user groups across the country.

In the global context, despite their developments in the eighties, commercial availability of Josephson junctions and SQUIDs has started only recently and the applications are expected to proliferate. After the advent of High Temperature Superconductors (HTS), much effort has been devoted to development of HTS SQUIDs operating at liquid nitrogen temperatures; this has recently been extensively reviewed[22]. However, quite a few of the applications still rely on Nb–AlO_x–Nb Josephson junctions because of the relatively poor superconducting and other properties of HTS. The indigenous availability of Nb–AlO_x–Nb Josephson junctions and SQUIDs should, therefore, go a long way in establishing beneficial technologies in a number of important application areas.

1. Radhakrishnan, T. S., Janawadkar, M. P., Gireesan, K., Baskaran, R., Rita Saha and Vaidhyanathan, L. S., in *Advances in Superconductivity, New Materials, Critical Currents and Devices* (eds Pinto, R., Malik, S. K., Grover, A. K. and Ayyub, P.), New Age International (P) Ltd, 1996, pp. 199–204.
2. John Clarke, in *The New Superconducting Electronics* (eds Weinstock, H. and Ralston, R. W.), Kluwer, Dordrecht, 1993, pp. 123–180.
3. Hans Koch, in *Sensors – A Comprehensive Survey* (eds Boll, R. and Overshott, K. J.), VCH Publishers, NY, 1989, vol. 5, pp. 381–445.
4. Tesche, C. D. and Clarke, J., *J. Low Temp. Phys.*, 1977, **29**, 301–331.
5. Ketchen, M. B. and Jaycox, J. M., *Appl. Phys. Lett.*, 1982, **40**, 736–738.
6. Simon, W., Liebmann, E. K., Simon, M. and Bucher, E., *J. Appl. Phys.*, 1992, **72**, 4474–4476.
7. Janawadkar, M. P., Baskaran, R., Gireesan, K., Rita Saha, Vaidhyanathan, L. S. and Radhakrishnan, T. S., *Jpn. J. Appl. Phys.*, 1994, **33**, L1662–L1664.
8. Sachslehner, F. and Vodel, W., *Cryogenics*, 1998, **38**, 293–298.
9. Safar, H., Gammel, P. L., Bishop, D. J., Mitzi, D. B. and Kapitulnik, A., *Phys. Rev. Lett.*, 1992, **68**, 2672–2675.
10. Greenberg, Ya. S., *Rev. Mod. Phys.*, 1998, **70**, 175–222.
11. Michelson, P. F., Price, J. C. and Taber, R. C., *Science*, 1987, **237**, 150–157.
12. Cabrera, B., *Phys. Rev. Lett.*, 1982, **48**, 1378–1381.
13. Le Gros, M., Da Silva, A., Turrell, B. G., Kotlicki, A. and Drukier, A. K., *Appl. Phys. Lett.*, 1990, **56**, 2234–2236.
14. Clarke, J., Gamble, T. D., Goubau, W. M., Koch, R. H. and Miracky, R. F., *Geophys. Prospect.*, 1983, **31**, 149–170.
15. Arnold Orange, S., *Proc. IEEE*, 1989, **77**, 287–317.
16. Hamalainen, M., Hari, R., Ilmoniemi, R. J, Knuutila, J. and Lounasmaa, O. V., *Rev. Mod. Phys.* 1993, **65**, 413–497.
17. Carelli, P. and Pizzella, V., *Supercond. Sci. Technol.*, 1992, **5**, 407–420.
18. Wiskswo, J. P. Jr., *IEEE Trans. Appl. Supercond.*,1995, **5**, 74–120.
19. Jenks, W. G., Sadeghi, S. S. H. and Wikswo, J. P. Jr., *J. Phys. D*, 1997, **30**, 293–323.
20. Fraser Neil, *New Sci.*, 1996, 24–27.
21. Czipott, P. V. and Podney, W. N., *IEEE Trans. Mag.*, 1989, **25**, 1204–1207.
22. Koelle, D., Kleiner, R., Ludwig, F., Dantsker, E. and John Clarke., *Rev. Mod. Phys.*, 1999, **71**, 631–686.

ACKNOWLEDGEMENTS. This paper is a result of intensive work in a project carried out during the course of about seven to eight years. We thank Dr P. K. Iyengar and Mr C. V. Sundaram for responding to our enthusiasm and supporting the establishment of this capital-intensive programme. We thank the Department of Science and Technology, Government of India for their role in promoting the applications of superconductivity in India and Dr R. Chidambaram, Dr Placid Rodriguez and Dr Baldev Raj for their sustained support and encouragement. We thank Dr Y. Hariharan for his association in the establishment of the device laboratory and for many helpful discussions, and Mr M. K. Ranganathan, Ms G. Chinnamma, Ms R. Mallika, Mr N. Thiruarul and Mr N. Chinnaswamy for rendering valuable technical assistance during the entire course of the work.

Received 19 June 1999; revised accepted 22 July 1999